International Journal of Pharmaceutics 686 (2025) 126369

Contents lists available at ScienceDirect

International Journal of Pharmaceutics

journal homepage: www.elsevier.com/locate/ijpharm

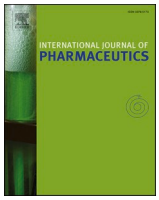

Choline chloride–malic acid Natural Deep Eutectic Solvent containing hydrophobic drugs: Insights into solubility and permeability behavior in digestive tract models

Stefano Sangiorgi [a], Matilde Mancinelli [a,c], Serena Bertoni [a], Massimiliano Pio Di Cagno [b,c], Nadia Passerini [a], Beatrice Albertini [a,*]

[a] University of Bologna, Dep. of Pharmacy and BioTechnology, Via San Donato 19/2 I-40127, Italy
[b] University of Trieste, Dep. of Chemical and Pharmaceutical Sciences, P.le Europa 1, I-34127, Italy
[c] University of Oslo, Dep. of Pharmacy, Sem Sælands vei 3, 0371 Oslo, Norway

ARTICLE INFO

Keywords:
Eutectic solvents
BCS Class II drugs
Solubility enhancement
Supersaturation
Permeation
Biorelevant media

ABSTRACT

This study evaluated the biopharmaceutical performance of six BCS Class II drugs with diverse physicochemical properties, formulated in a Natural Deep Eutectic Solvent (NaDES) composed of choline chloride and malic acid (1:1 M ratio). The selected APIs included weak bases (domperidone, cinnarizine, olanzapine), weak acids (nimesulide, flurbiprofen), and a pH-independent compound (carbamazepine). Solubility assessments revealed a 5- to 70-fold increase in API solubility in NaDES compared to biorelevant digestive media. In vitro dilution studies in FaSSGF and FaSSIF demonstrated that NaDES facilitated the formation of supersaturated drug solutions at critical pH levels, particularly for carbamazepine and weakly basic APIs with log P $\leq$ 4. Conversely, cinnarizine (log P > 5.5) failed to maintain the supersaturated state, likely due to its pronounced hydrophobicity and limited hydrogen bonding capacity with the NaDES components. Under gastric conditions, weakly acidic APIs approached their solubility limits; however, all API + NaDES formulations exhibited superior solubilization kinetics compared to conventional solid dosage forms. Permeability studies using biomimetic Permeapad® barriers in PBS, FaSSIF and FeSSIF confirmed enhanced performance for neutral and basic drugs, but not for acidic ones. These findings highlight the potential of choline chloride–malic acid NaDES as a green and effective drug delivery platform. Nevertheless, its ability to improve bioavailability is highly dependent on the molecular characteristics of each API + NaDES system. Upon dilution in biorelevant media, performance is governed by a delicate interplay of hydrogen bonding, hydrophobic interactions and competition with solubilizing agents present in gastrointestinal fluids.

1. Introduction

Oral administration is the preferred route for delivering therapeutic agents, especially in chronic treatments. To improve drug bioavailability, different bottom-up and top-down processing techniques are used to enhance the solubility of poorly water-soluble drugs (Bhalani et al., 2022; Alqahtani et al., 2021; Milián-Guimerá et al., 2023). From a sustainability standpoint, employing simple solvents to enhance the biopharmaceutical properties of therapeutic molecules offers significant advantages, such as reduced environmental impact and lower production costs. Over the past decade, ionic liquids (ILs) and deep eutectic solvents (DESs) have emerged as innovative, greener alternatives to conventional organic solvents. These novel solvents are highly versatile and have demonstrated the ability to enhance drug solubility and, in some cases, bioavailability (Banerjee et al., 2018; Peng et al., 2021). Numerous studies have reviewed their unique physicochemical properties, synthesis methods, and wide-ranging applications across various fields, including materials science and pharmaceutics (Dai et al., 2015; Liu et al., 2022; Moshikur et al., 2023; Sangiorgi et al., 2025; Zhuo et al., 2024).

Natural DESs (NaDESs) represent a greener, safer and more cost-effective alternative to ILs and DESs (Zainal-Abidin et al., 2019). The primary components used in the formation of NaDESs are non-synthetic molecules such as choline chloride (ChCl), betaine, polyols,

* Corresponding author.
E-mail address: beatrice.albertini@unibo.it (B. Albertini).

https://doi.org/10.1016/j.ijpharm.2025.126369
Received 9 September 2025; Received in revised form 3 November 2025; Accepted 5 November 2025
Available online 9 November 2025

carbohydrates, amides, amines, alcohols, and carboxylic acids, which act as potential hydrogen bond acceptors (HBAs) or hydrogen bond donors (HBDs). These components are usually selected through a trial-and-error approach, which involves systematically testing various combinations of HBDs and HBAs to identify the most stable eutectic mixtures with desirable physicochemical properties. NaDES offer many advantages over ILs and DESs such as high biodegradability, low volatility, low production costs, low toxicity, and high biocompatibility, which fully represent the green chemistry metrics (Omar and Sadeghi, 2022; Smith et al., 2014).

Over the past decade, numerous studies have demonstrated the effectiveness of NaDESs in enhancing the solubility of various small molecules belonging to BCS classes II and IV, as well as high molecular weight natural products (as summarized by the comprehensive review from Sangiorgi et al., 2025). Drug-NaDES systems have been shown to consist of a complex supramolecular structure influenced by factors such as water content in binary/ternary mixtures, hydrogen bonding, and hydrophobic interactions (Albertini et al., 2023). In terms of drug solubilization, two possible mechanisms have been proposed: the liquid crystal theory and the binding theory (Sangiorgi et al., 2025).

At this stage, there have been limited studies investigating the drug release from eutectic formulations in the gastrointestinal (GI) fluids media and/or drug permeation across biological membranes. Recently, Jeliński et al. (2019) evaluated the behavior of curcumin- loaded NaDES composed by ChCl and glycerol at a 1:1 M ratio. Specifically, curcumin solubility in NaDES was found to be 3.5 times higher than in FaSSGF and 2 times higher than in FaSSIF. Quantum chemistry computations indicated that direct intermolecular bonds forming hetero-molecular pairs with ChCl and Gly were responsible for elevating the bulk concentration of curcumin. However, diluting the drug-loaded NaDES with larger volumes of GI fluids led to reduced curcumin solubility and delivery compared to smaller dilution volumes. Palmelund and colleagues (Palmelund et al., 2021) used ChCl and levulinic acid (at 2:1 M ratio) based NaDES to enhance the bioavailability of the model drug aprepitant. The in vitro drug release in FaSSIF dissolution medium revealed a higher percentage of drug release from the eutectic solvents compared to the amorphous form. Consistent with the drug release results, the in vitro permeation study showed that these formulations resulted in the highest fraction of drug permeation, followed by the amorphous and nanocrystalline commercial formulations. Despite promising in vitro results, the NaDES formulation did not show improved in vivo performance in rats compared to the nanocrystalline formulation, although it had higher oral bioavailability than amorphous aprepitant.

Different ChCl-based NaDESs were also tested for celecoxib solubility enhancement (Chakraborty et al., 2023); among them ChCl and malonic acid based NaDES achievied an increase of up to 10,000 times compared to the drug solubility in deionized water. In vitro drug release in FaSSIF initially showed high supersaturation, which declined by approximately two-fold after 2 h. Moreover, pharmacokinetic analysis revealed that the NaDES consistently improved drug bioavailability compared to the neat crystalline drug. Finally, the intestinal absorption of daptomycin was assessed using a NaDES formulation as an oral permeation enhancer, compared to the well-known enhancer sodium caprate. Diffusion studies highlighted the capacity of ChCl-Gly-based DES to modulate the tight junctions of intestinal epithelial cells, thereby promoting GI drug absorption (Saiswani et al., 2023).

NaDES can be formulated using components that are either in the liquid or solid state at room temperature. However, in the authors' opinion, the use of a liquid component, whether acting as HBA or HBD, may complicate the interpretation of results where the aim is to evaluate the solubilizing capacity of NaDES. This is because such components, including glycerol, ethylene/propylene glycol, glycolic acid, and lactic acid, are known to act as effective solvents for poorly water-soluble APIs independently (Albertini et al., 2024; Li and Lee, 2016; Mustafa et al., 2021). In contrast, solid components offer a more reliable basis for eutectic systems. Among these, choline chloride is the most commonly used HBA, while sugar alcohols (e.g., glucose, xylitol, sorbitol) and polycarboxylic acids (e.g., citric, malic and malonic acids) are frequently employed as HBDs (Morrison et al., 2009; Sut et al., 2017; Cysewski and Jeliński, 2019; Albertini et al., 2023).

This study aimed to provide a comprehensive evaluation of NaDES + BCS Class II drug systems following oral administration, with particular emphasis on how dilution in various GI fluids affects drug solubility and membrane permeability. Through a stepwise experimental approach, the solubilizing efficiency of NaDES was thoroughly investigated, offering insights into their potential and limitations in drug delivery applications. To this end, a NaDES composed of choline chloride and malic acid was selected, based on its well-characterized solid–liquid equilibrium phase diagram (Martins et al., 2019), structural stability (Hammond et al., 2017), and proven ability to enhance the solubility of hydrophobic drugs (Albertini et al., 2023; Faggian et al., 2016).

The study includes a selection of BCS Class II drugs, characterized by poor solubility but high permeability, with diverse physicochemical properties such as logP, solubility in physiological buffers, melting point, and pKa. Specifically, domperidone (DOM), cinnarizine (CIN), and olanzapine (OLZ) were chosen as weakly basic drugs; nimesulide (NIM) and flurbiprofen (FLU) as weakly acidic drugs; and carbamazepine (CBZ) as a pH-independent compound. The API + NaDES mixtures were first assessed for solubility enhancement compared to simple buffer solutions (pH 1.2 and 6.8), followed by evaluation in biorelevant media simulating fasted gastric and intestinal conditions (FaSSGF – pH 1.6 and FaSSIF – pH 6.5). Their behavior upon dilution in these media was then analyzed and compared with the dissolution profiles of pure APIs and conventional solid dosage forms (tablets or granules). Finally, in vitro permeation studies were conducted using PermeaPad® biomimetic membranes under both fasted and fed conditions (FaSSIF – pH 6.5 and FeSSIF – pH 5).

2. Experimental section

2.1. Materials

ChCl (purity ≥ 98 %, MW = 139.62 g/mol), Malic acid (MA) (≥95 %, MW = 134.09 g/mol), sodium chloride (≥99 %, MW = 58.44 g/mol), Potassium chloride (≥99 %,MW = 74.55 g/mol), hydrochloric acid (37 %, MW = 36.46), sodium phosphate tribasic (≥99.9 %, MW = 163.94 g/mol), potassium phosphate monobasic (≥99.9 %, 136.09 g/mol), ammonium acetate (≥98 %, MW = 77.08 g/mol), acetic acid (MW = 60.05 g/mol), sodium hydroxide (≥97 %, MW = 40 g/mol), L-α-phosphatidylcholine (~60 %), sodium taurocholate hydrate (≥97 %, MW = 537.68 g/mol), sodium phosphate monobasic dihydrate (≥99 %, MW = 156.00 g/mol) and disodium hydrogen phosphate dihydrate (≥98 %, MW = 177,99 g/mol) were purchased from Sigma Aldrich (Steinheim, Germany). Maleic acid (≥99 %, MW = 116.07 g/mol) was obtained from Fluka (Steinheim, Germany). 3F powder (FFF02, 70 g), FaSSIF buffer concentrates (FASBUF, 250 g) and FeSSIF buffer concentrates (FESBUF, 250 g) were purchased from Biorelevant (London, United Kingdom). PermeaPad® GIT plate was purchased from Phabioc GmbH (Espelkamp, Germany). All other chemicals used for HPLC analysis were of analytical grade.

The APIs NIM, CIN, FLU, OLZ and CBZ were purchased from Sigma Aldrich. DOM was bought from A.C.E.F. s.p.a (PC, Italy).The characteristics of the selected APIs are reported in Table 1. Commercial oral solid dosage forms were obtained from the local pharmacy: Peridon® (DOM) 10 mg tablet (Italchimici, Milan, Italy); Cinazyn® (CIN) 25 mg divisible tablets (Italchimici, Milan, Italy); Aulin® (NIM) 100 mg granules (Angelini, Rome, Italy) and Olanzapine® DOC generici (OLZ) 10 mg tablets (DOC, Milan, Italy). For FLU and CBZ, no commercial oral solid dosage forms with suitable API amount were available; therefore, tablets with 5 mg of FLU or 30 mg of CBZ were manufactured adding 300 mg of the Meggle® Compaction Blend, composed by lactose monohydrate, cellulose powder, aluminium oxide and vegetable magnesium stearate.

Table 1
Structure and characteristics of selected BCS class II APIs.

APIs		Chemical structure	MW (g/mol)	pka	LogP	Melting point (°C)
Weak acids	FLU	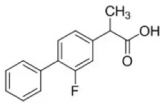	244.26	4.42[a]	4.16[a]	110–111[a]
	NIM	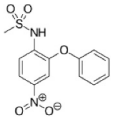	308.31	6.50[b]	2.60[b]	149[b]
Weak bases	CIN	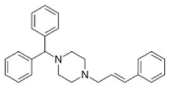	368.51	8.10[c]	5.88[c]	117–120[c]
	DOM	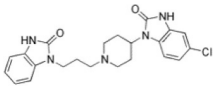	425.95	7.90[d]	3.90[d]	236–239[d]
	OLZ	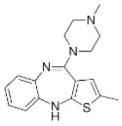	312.43	7.24[e]	4.09[e]	189–195[e]
pH independent	CBZ	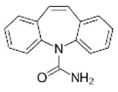	236.27	13.9[f]	2.77[f]	190–193[f]

[a] https://go.drugbank.com/drugs/DB00712.
[b] https://go.drugbank.com/drugs/DB04743.
[c] https://go.drugbank.com/drugs/DB00568.
[d] https://go.drugbank.com/drugs/DB01184.
[e] https://go.drugbank.com/drugs/DB00334.
[f] https://go.drugbank.com/drugs/DB00564.

The tablets (⌀ = 11 mm) were obtained by direct compression (Costamac GPX, LC, Italy) by applying a force of 8 tons for 3 min.

2.2. Solubility studies

The thermodynamic solubility, namely, the equilibrium solubility, of the APIs was measured in both buffer solutions (pH 1.2 and 6.8, prepared according to the Ph. Eur.) and biorelevant media, with the temperature set at 37 °C, as used in the dilution/dissolution tests. To evaluate the equilibrium solubility of each drug in buffers, an excess of API was added to 10 mL of buffer solution. The samples were magnetically stirred for 48 h, and the suspensions were centrifuged at 10,000 rpm for 20 min. The supernatants were suitably diluted in buffer solution before the analysis and detected by UV–Vis spectrophotometer. The analytical parameters used for each API are reported in Table S1. Each sample was analyzed at least in triplicate. The same determination was carried out using biorelevant media: Fasted State Simulated Gastric Fluid (FaSSGF) at pH 1.6 and Fasted State Simulated Intestinal Fluid (FaSSIF) at pH 6.5 prepared according to the literature (Vertzoni et al., 2010; Amaral Silva et al., 2022; Jantratid et al., 2008). After centrifugation, the supernatant was diluted in the mobile phase, filtered through 0.45 μm PTFE filters (Thermo Scientific, Rockwood, North America) and analyzed by HPLC-UV. The analytical specifications are shown in Table S1. Moreover, the solubility of the APIs in the NaDES system was evaluated adding an excess of each drug into 10 mL of the NaDES. The samples were magnetically stirred for 48 h and the suspensions were then centrifuged (Eppendorf Centrifugate 5810R) at 14,000 rpm for 20 min. The supernatants were suitably diluted and analyzed spectroscopically. Each sample was analyzed at least in triplicate.

2.3. API-loaded NaDES preparation

A NaDES based on a 1:1 M ratio mixture of ChCl and MA, with 5 % w/w H2O, was prepared by heating the solid at 70 °C until a clear and homogeneous solution was obtained. The liquid system was then allowed to cool to room temperature (RT). Each API was subsequently added in excess, following the procedure described for the API solubility studies in NaDES (Section 2.2). The prepared API + NaDES mixtures were then stored at RT, protected from light, for up to 12 months.

2.4. In vitro dilution and dissolution tests

The dilution tests performed in buffer solutions (pH 1.2 and 6.8) were assessed using a paddle apparatus in accordance with the current European Pharmacopoeia, rotating at 75 rpm and maintained at 37 °C. The system was connected to a peristaltic pump (Minipuls 3, Gilson, Milan, Italy), via silicone tubes, operating at a fixed flow rate of 5 mL/min to enable automated spectrophotometer readings. A polyethylene filter with a 10 μm pore size (Quality Lab Accessories, Telford, England) was placed at the end of the silicone tube to prevent solid particles from entering the solution drawn from the vessel. Measurements were taken every 5 min over a total period of 3 h, with the first hour conducted at pH 1.2 and the remaining two hours at pH 6.8. The tests were performed using a total volume of 500 mL. Initially, 360 mL of buffer solution at pH 1.2 was used, and after the first hour, 180 mL of a solution at pH 12.32 were added to achieve a final pH of 6.8. Due to the acidic nature of the NaDES (pH 1.5–2), the pH was adjusted adding a suitable amount of NaOH 0.1 M. The pH was monitored throughout the test using pH indicator strips. The final pH was then confirmed using a pH meter (XS

Instruments, Modena, Italy) at the end of the test.

The drug-loaded NaDESs were added at time zero in an adequate amount to have a drug concentration inside the vessel that is intermediate between the solubility of each drug at pH 1.2 and pH 6.8 to create a supersaturated environment at the unfavorable pH for each drug. Thus, the dissolution was performed in sink conditions in the favorable pH environment, and non-sink conditions in the unfavorable pH. The Sink Index (SI) was used to express the extent of non-sink conditions (Bertoni et al., 2023; Schver and Lee, 2021), calculated as follow:

$$SI = Cs/(\text{Dose/V}) \quad (1)$$

Where Cs is the solubility of crystalline drug in the specific fluid, V the volume of the dissolution medium and Dose the total amount of drug in the test sample. The tests were carried out at least in triplicate.

Small-scale dilution tests were then performed using biorelevant media (Fig. S1) under simulated fasted state conditions, proportionally reducing the volumes of gastric and intestinal fluids, and considering the addition of water as the medium for drug administration in accordance with scientific literature (Culen et al., 2013). Specifically, at time zero, an appropriate amount of loaded NaDES was added to a vessel containing 50 mL of water and 12 mL of FaSSGF at pH 1.6 at 37 °C to simulate the gastric phase. After one hour, 38 mL of FaSSIF was added into the vessel and the test was performed for other 2 h to mimic the intestinal phase. The pH was then adjusted at pH 6.5 adding a suitable amount of NaOH 0.1 M. At predetermined time-points (1, 5, 15, 30, 60, 65, 75, 90, 120, 150 and 180 min), 2 mL samples were collected, appropriately diluted with the mobile phase, and filtered with PTFE filters 0.2 μm (Thermo Scientific, Rockwood, North America) before to be analyzed by HPLC-UV. As in the case of buffers, it was then necessary to correct the pH by adding an appropriate volume of 1 M NaOH. Additionally, for both buffer solutions and biorelevant media, the dilution profiles of the loaded NaDESs were compared with the dissolution profiles of pure drugs and solid dosage forms.

2.5. Permeability tests

APIs permeability was investigated using the high-throughput 96-well PermeaPad® plate (di Cagno et al., 2015). For each drug, two samples were analyzed: the loaded NaDES diluted 1:5 in PBS/FaSSIF/FeSSIF, respectively, and a suspension of each drug powder prepared weighing the same amount of drug considered in loaded NaDES test and adding it to 5 mL of PBS/FaSSIF/FeSSIF. The donor and acceptor plates of the PermeaPad® GIT Plate were separated; each acceptor well was filled with 400 μL PBS and the donor plate was set back into bottom one; the donor wells were then filled with 200 μL of the samples. Moreover, the plate was sealed with transparent adhesive sealing foil and placed on the orbital shaker plate and secure in place. The plate was incubated in an orbital shaker-incubator (ES-20, Biosan, Riga, Latvia) at 37 °C and agitated at 200 rpm for 4 h. Samples of 100 μL were withdrawn from the acceptor compartment every hour and replaced with fresh PBS.

Drug concentrations in the samples were determined by spectrophotometric measurements on a Spectramax 190 Microplate Reader (Molecular Devices Inc., Sunnyvale, California, USA) at drug-specific wavelengths. Experiments were repeated at least in triplicate. The results were expressed as in vitro fraction of dose absorbed (F_{abs}, %) calculated from the drug flux determined using the PermeaPad® device, as shown in Eq. (2).

$$\text{Fabs } (\%) =) = \frac{\mu mol4h}{\text{administered dose}} x100 \quad (2)$$

where μmol_{4h} represents the moles of drug in the acceptor compartment after 4 h, calculated by multiplying the concentration obtained from the interpolation of the absorbance on the calibration curve by the volume of the acceptor compartment (400 μL), while administered dose represents the amount of drug in the donor compartment at the beginning of the test.

Phosphate-buffered saline (PBS) preparation – PBS buffer 73 mM (pH 7.4) was obtained mixing one part of a 2.5 % (w/v) sodium phosphate monobasic dihydrate solution with four parts of a 0.9 % (w/v) disodium hydrogen phosphate dihydrate solution. Then the pH was measured with SevenCompact pH/ion meter S220 (Mettler Toledo Columbus, Ohio, USA) and adjusted to 7.40 ± 0.05 by the addition of NaOH pellets. The tonicity of the solution was measured using Semi Micro Osmometer K-7400 (Knauer, Berlin, Germany) and adjusted to 280–300 mOsm/kg with NaCl. Finally, the PBS solution was filtered with 0.2 μm filter (Whatman® Nuclepore Track-Etch membrane filter; GE Healthcare Life Sciences, Maidstone, UK).

Intestinal simulated fluid preparation – FaSSIF and Fed State Simulated Intestinal Fluid (FeSSIF) were prepared using 3F Powder, FaSSIF/FeSSIF Buffer Concentrate and distilled water. The preparation of 250 mL of FaSSIF (pH 6.5) consists of weighing 10.41 g of FaSSIF Buffer Concentrate and 240.3 g of purified water. Then, 0.560 g of 3F Powder was added and the solution was prepared stirring until the powder was totally dissolved. In the end, it was necessary to let the solution equilibrate for two hours before using it. In order to prepare 250 mL of FeSSIF (pH 5.0), 20.35 g of FeSSIF Buffer Concentrate and 229.8 g of purified water were weighed. Then, 2.800 g of 3F Powder was added and the solution was prepared stirring until the powder completely dissolved.

2.6. APIs analysis

2.6.1. Quantification of the APIs in the solubility and dilution/dissolution tests

The spectrophotometric analysis was performed using a Cary 60 UV–Vis spectrophotometer from Agilent Technologies (Waldronn, Germany). A stock solution of 1 mg/mL for each drug was prepared in ethanol and used to obtain calibration curves at pH 1.2 and 6.8. The conditions for quantifying the APIs are reported in Table S1.

The HPLC system consisted of two mobile phase delivery pumps (LC-10ADvp, Shimadzu, Kyoto, Japan), a UV–Vis detector (SPD-10Avp, Shimadzu, Kyoto, Japan) and an autosampler (SIL-20 A, Shimadzu, Kyoto, Japan). All tests were carried out at least in triplicate. The conditions for quantifying the various APIs dissolved in the biorelevant media are detailed in Table S1. For all methods, the injected volume was 20 μL, and the chromatographic run followed an isocratic method with a mobile phase flow rate of 1 mL/min. For the calibration curve, a stock solution (1 mg/mL) of each API was prepared by dissolving 10 mg of API in 10 mL of acetonitrile. The stock solution was then diluted with the mobile phase to prepare solutions at various API concentrations, which were injected.

2.6.2. Quantification of the APIs in permeability tests

The analysis of the amount of permeated drug was performed using a Spectramax 190 Microplate Reader. A stock solution of 1 mM in PBS for FLU and OLZ, and 4 mM in EtOH for the other four APIs, was used to obtain calibration curves in PBS. The conditions for quantifying the APIs in PBS are shown in Table S1.

2.7. Statistical analysis

Statistical analysis was performed with two-way analysis of variance (ANOVA) followed by the Bonferroni posthoc test (GraphPadPrism, GraphPad software, Inc., San Diego, CA, USA).

3. Results and discussion

The NaDES used in this study was a eutectic mixture of ChCl and MA in a 1:1 M ratio, containing 5 % w/w of H_2O. Water was added to reduce viscosity, improve solvent handling and shorten the preparation time (Albertini et al., 2024, 2023). The resulting NaDES appeared as a liquid at RT, homogeneous and clear.

3.1. Solubility studies of APIs in gastrointestinal fluids and NaDES

The results of the solubility studies carried out in buffer solutions and biorelevant media are reported in Fig. 1.

Being weak acids, NIM and FLU exhibited greater solubility at pH 6.8 than at pH 1.2. At pH 6.8, the sulfonamide group of NIM and the carboxyl group of FLU are deprotonated, which enhanced their solubility. As expected, the weak bases (DOM, CIN, OLZ) resulted more soluble at pH 1.2 than at pH 6.8, in fact at pH 1.2, the protonated N-piperazine moiety of OLZ and CIN contributed to their enhanced solubility. Similarly, DOM has the nitrogen of the piperidine ring protonated. Finally, CBZ, a pH-independent drug, showed equal solubility at both pH levels, consistent with the pKa (see Table 1).

The APIs solubility in FaSSGF and in FaSSIF was overall enhanced by the presence of solubilizing agents, such as L-α-phosphatidylcholine and sodium taurocholate, able to form micellar structures. In fact, NIM showed a slight increase in solubility in biorelevant media compared to buffers (Fig. 1A), however this difference was not significant ($p > 0.05$). In contrast, the other weak acid, FLU, showed a significant solubility enhancement in FaSSIF compared to the buffer at pH 6.8 (Fig. 1B). The solubility values of DOM resulted more than doubled in both FaSSGF and FaSSIF compared to buffer solutions (Fig. 1C). A similar trend was observed for CIN at acidic pH (Fig. 1D). However, in the intestinal environment, CIN's solubility remained very low, with no statistically significant differences between buffer pH 6.8 and FaSSIF.

An opposite trend was observed for OLZ (Fig. 1E): the drug exhibited

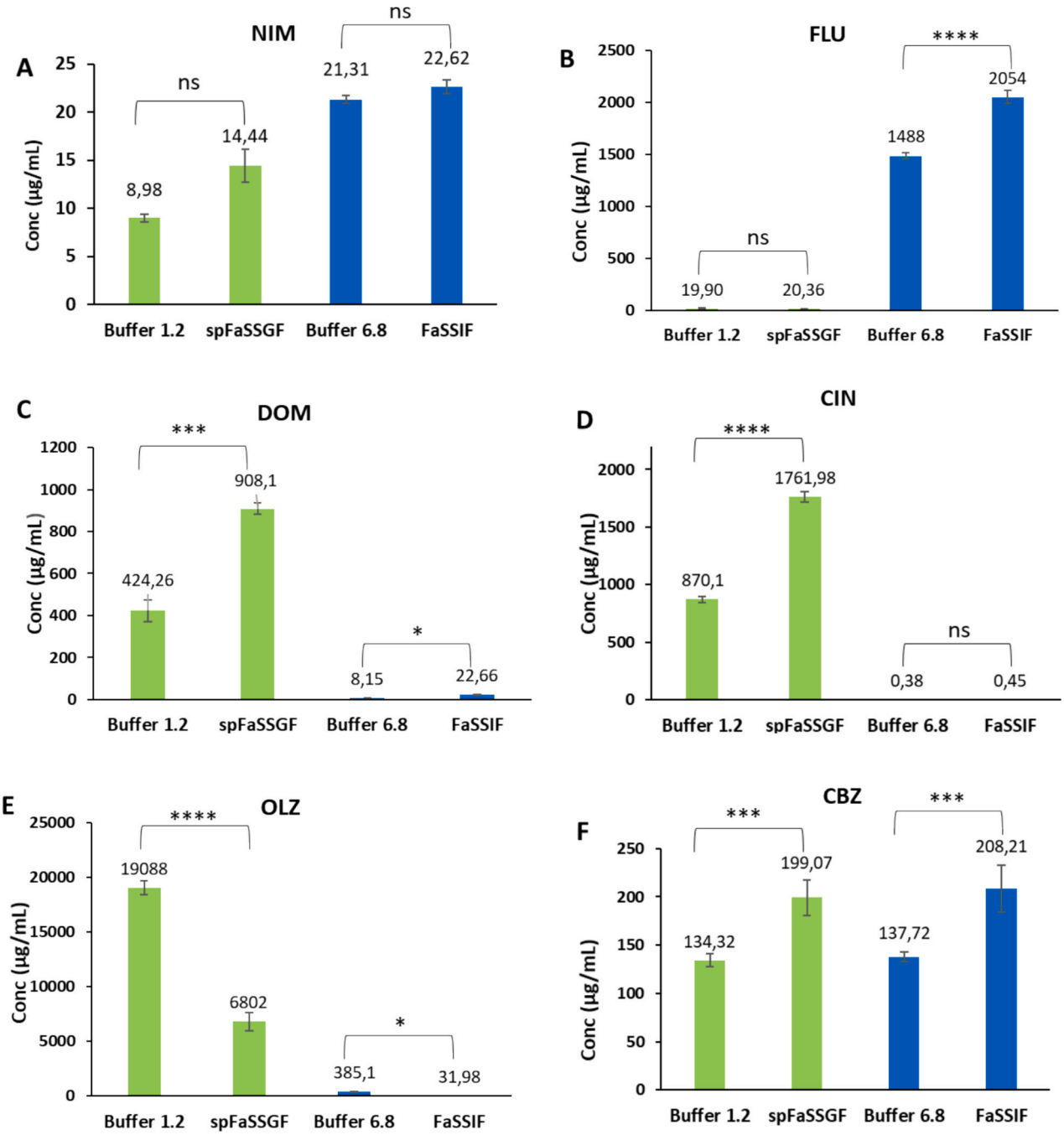

Fig. 1. Comparison of equilibrium solubility values in buffers and biorelevant media of the APIs under investigation. Values are expressed as mean (n = 3) ± SD. *p < 0.05; *** p < 0.001; **** p < 0.0001, significant difference.

higher solubility in buffer solutions compared to biorelevant media, with solubility decreasing approximately threefold in FaSSGF and twelvefold in FaSSIF, respectively. This suggests that for some weakly acidic or weakly basic drugs, biorelevant media do not always enhance solubility compared to simple buffer solutions. For example, flurbiprofen solubility is significantly higher in phosphate buffer pH 6.8 (~3127 μg/mL) than in the biorelevant medium FaSSIF (~1585 μg/mL), likely due to its strong pH-dependent solubility and limited interaction with bile salt micelles (Loisios-Konstantinidis et al., 2020).

Finally, CBZ showed greater solubility in both FaSSGF and FaSSIF compared to buffer solutions. This behavior confirms that the presence of surfactant species in biorelevant media generally promotes the solubilization of poorly water-soluble drugs (Fig. 1F).

Regarding the solubility of the APIs in the selected NaDES, the results evidenced a significant increase (****$p < 0.0001$), ranging from 1.5- to 80-fold, compared with their maximum solubility values in biorelevant media (Table 2). As expected, the APIs that exhibited the greatest solubility were the weak bases (OLZ, DOM and CIN). These results align with Chakraborty *et* al. (Chakraborty et al., 2023), who reported that a ChCl: malonic acid (1:1 M ratio) NaDES induced hydrotropic solubilization of aprepitant, a weak acid BCS class II drug with a log P = 3.5, particularly in biorelevant media. In contrast, the acidic drugs (NIM and FLU) exhibited low absolute solubility values. However, considering their inherently poor aqueous solubility, the enhancement observed for NIM was particularly notable, reaching up to a 70-fold increase (Table 2). CBZ showed a solubility in NaDES intermediate between that of weak acids and weak bases.

3.2. Post-Ingestion dilution behavior of APIs + NaDES systems in gastrointestinal fluids

3.2.1. Preliminary evaluation using simple buffers and biorelevant media

Dilution studies were performed in simulated gastrointestinal fluids (both simple buffers and biorelevant media) by adding either the drug + NaDES system or the pure drug to generate a supersaturated environment at the unfavorable pH for the API. NIM and DOM were selected as representative weak acid and weak base, respectively.

For NIM, a concentration of 15 μg/mL was chosen to achieve an intermediate value between the drug's solubility at pH 1.2 and pH 6.8 (Fig. 1A). This created a supersaturated condition at pH 1.2 (C = 2Cs), allowing the evaluation of the drug's behavior under unfavorable pH conditions. As shown in Fig. 2A, the raw drug exhibited slow solubilization kinetics, reaching only about 40 % of the total concentration after 3 h. In contrast, NIM + NaDES system enabled rapid drug solubilization with approximately 50–55 % of the total amount solubilized, which is close to its equilibrium solubility in that medium (calculated considering the solubility data in this medium, Fig. 1). Upon pH change, the solubilization of pure NIM continued slowly, eventually reaching a plateau at 35 %. In contrast, the NaDES formulation achieved complete solubilization of NIM, and this condition was maintained until the end of the test, underlining the capability of NaDES to re-solubilize precipitated NIM.

For dilution studies in biorelevant media, the concentration of NIM was set at 20 μg/mL. Similar to its behavior in buffers, the pure drug (Fig. 2A) exhibited slow solubilization rates in FaSSGF; however, it reached a higher concentration (35 % of the total in FaSSGF compared to 12 % at pH 1.2) due to the presence of solubilizing species. On the contrary, the NaDES formulation reached the drug equilibrium solubility within 5 min and this condition was maintained throughout the gastric phase. Following the pH shift, the solubilized NIM fraction increased in both profiles, reaching a plateau at around 70 % of the administered dose after 90 min. For the pure drug, the extent of solubilization was higher than that observed in buffer solutions. However, during the intestinal phase, the solubilization of NIM remained incomplete, likely because the drug concentration approached its maximum solubility in FaSSIF. This is consistent with the similar solubility values observed in both simulated fluids (Table 2), a behaviour attributable to the slightly acidic nature of NIM, which makes it behave almost like a pH-independent compound. NaDES were able to maintain NIM in solution at concentrations close to its solubility, even under acidic conditions. Nevertheless, the solubilized drug amount was lower in FaSSIF compared to phosphate buffer at pH 6.8, suggesting competing mechanisms of drug precipitation and hydrotropic solubilization.

For DOM, the concentration of 50 μg/mL was used to ensure sink conditions in acidic solution and supersaturated state at pH 6.8 (C = 6Cs), in order to evaluate the behavior of the NaDES formulation under the most critical conditions (pH = 6.8). The raw drug profile (Fig. 2B) demonstrated slow solubilization kinetics at both pH levels. However, after NaDES formulation dilution with the acidic fluid, the drug was completely solubilized within 15 min, despite DOM + NaDES being diluted by more than 30 %, which is the dilution concentration at which the breakdown of the hydrogen bond network was observed (Rozas et al., 2021). This supersaturated state was sustained until the end of the test (up to two hours), likely due to slow precipitation kinetics. The behavior of the loaded NaDES in biorelevant media was evaluated using the same DOM concentration as in the buffer tests. Unlike what was observed in buffers, the profiles of the raw API and the loaded NaDES were superimposable, achieving complete solubilization of the drug within 5 min. The behavior of the raw drug is likely due to the components of the biorelevant media, which promote micellar solubilization of pure DOM, significantly enhancing powder dissolution. In the intestinal fluid, both profiles were similar displaying a slow precipitation process of this API.

Considering the results obtained, it is evident that simple buffer solutions might not adequately represent the behavior of the drug or drug + NaDES systems in the gastrointestinal environment. In contrast, biorelevant media offer a more realistic model for studying the biopharmaceutical properties of the API. Therefore, the study of the remaining drug + NaDES systems was carried out exclusively in biorelevant media.

3.2.2. Assessment of the dilution behavior in biorelevant media

The performances of the NaDES loaded with the different APIs were compared to dissolution profiles of both neat drugs and solid dosage forms (i.e., tablets or granules). Specifically, the dissolution behavior of commercial pharmaceutical formulations was assessed for DOM, CIN, NIM and OLZ. For FLU and CBZ, the dosages in the market formulations did not align with the concentrations chosen for the tests. Therefore, tablets with these APIs were prepared in the laboratory as previously described in the experimental section. The specific concentration of APIs and the Sink Index in the gastric and intestinal environments relative to the dilution studies are reported in Table 3.

The dilution profiles of the tested APIs in the biorelevant media simulating the fasted state under non-sink conditions mimicking in vivo administration are shown in Fig. 3.

3.2.3. Weak acid drugs (NIM & FLU)

For NIM (Fig. 3A), the commercial granules achieved a drug concentration of approximately 40 % within 20 min in FASSGF, although this was significantly lower than the NaDES sample. In FaSSIF, its behavior was similar to that of raw NIM, highlighting the potential advantage of NIM + NADES for improving systemic absorption.

Table 2
Equilibrium solubility (mg/mL) ± SD of the APIs in biorelevant media and in the NaDES.

APIs	FaSSGF	FaSSIF	NaDES	Increase
NIM	0.014 ± 0.002	0.023 ± 0.007	**1.61 ± 0.29**	>70
FLU	0.020 ± 0.002	2.053 ± 0.612	**3.46 ± 0.30**	>1.5
DOM	0.908 ± 0.027	0.023 ± 0.002	**29.07 ± 0.92**	>30
CIN	1.762 ± 0.046	0.005 ± 0.001	**21.48 ± 0.35**	>12
OLZ	6.802 ± 0.822	0.032 ± 0.002	**32.21 ± 0.40**	>5
CBZ	0.199 ± 0.018	0.208 ± 0.024	**12.91 ± 1.43**	>65

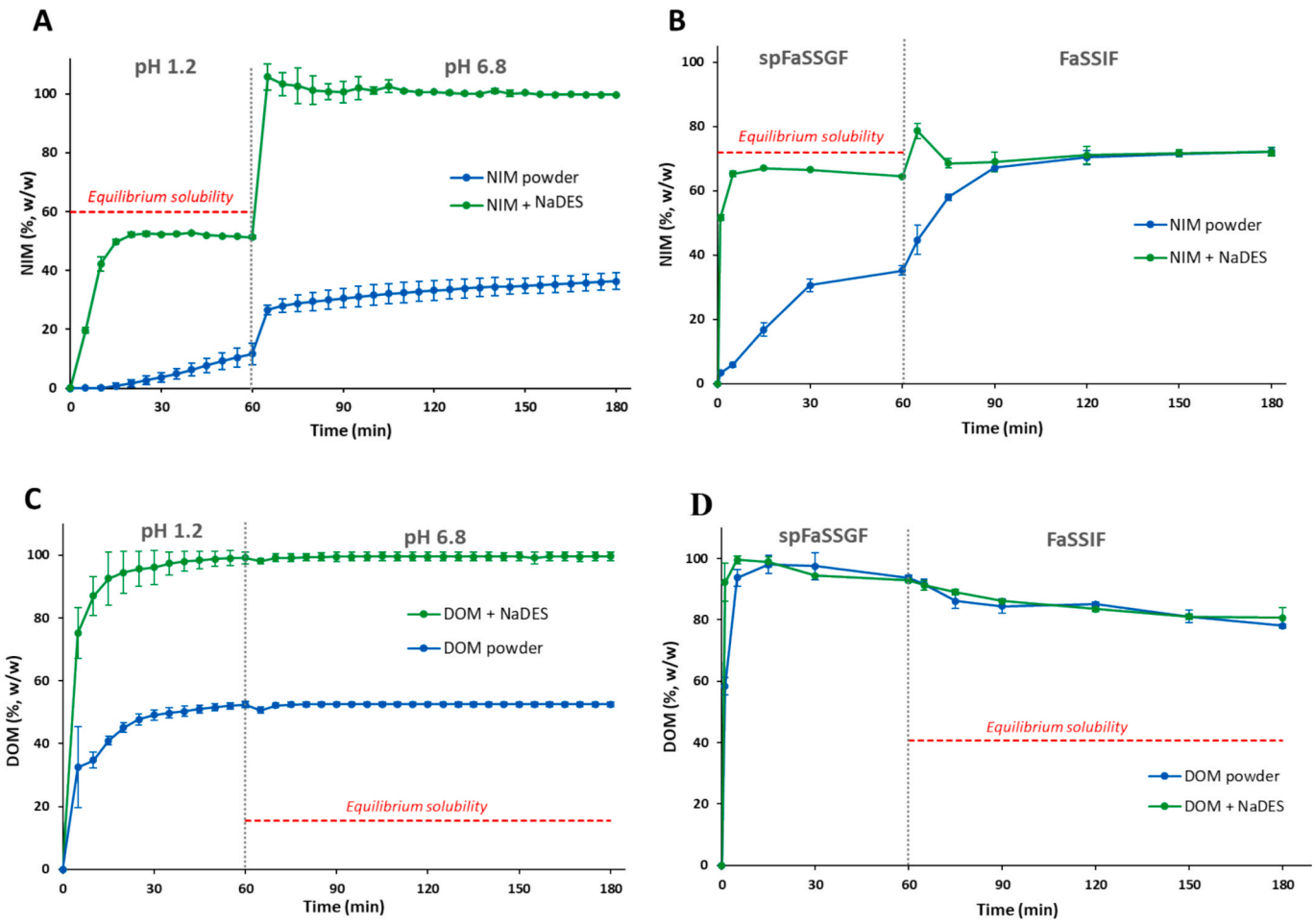

Fig. 2. Dilution profiles of NaDES containing A) the weak acid NIM in buffer solutions and B) in biorelevant media; and C) the weak base DOM in buffer solutions and D) in biorelevant media, compared to the dissolution profiles of pure drug. Values are expressed as mean (n = 3) ± SD in % of the total. The vertical grey line indicates the time at which the pH change was made. The dashed red lines indicate the equilibrium solubility of the neat drug in the specific dissolution medium.

Table 3
Experimental conditions (drug theoretical concentration, SI in the two media) used in the dilution tests for each drug compound. Generally, sink conditions are achieved when SI > 3, whereas non-sink conditions when SI < 1.

APIs		Conc used (μg/ml)	Sink Index (SI)	
			spFaSSGF	FaSSIF
Weak acids	FLU	50	0.4	41.1
	NIM	20	0.7	1.2*
Weak bases	CIN	50	18.2	0.5
	DOM	50	35.2	0.1
	OLZ	500	13.6	0.1
pH independent	CBZ	300	0.4	0.7

* Not proper sink conditions since NIM solubility in FaSSIF is slightly lower than Dose/V.

Moving to FLU (Fig. 3B), the pure drug and the tablet showed slow solubilization rates during the gastric phase; after the pH change, the drug continued to dissolve, eventually reaching a stable concentration value at approximately 90 % and 80 % of the total amount, respectively. As for NIM, the loaded NaDES reached a concentration near its equilibrium solubility within 5 min. Subsequently, FLU partially recrystallized up to a concentration of around 30 % of the whole amount. After the medium change, the drug was completely solubilized within 5 min and this condition was maintained until the end of the test. These results demonstrated NaDES's ability to maintain the drug in solution, even under challenging pH conditions. Although drug recrystallization was not avoided, it was slowed down by the NaDES. The recrystallized drug is likely to form small crystals, which enhance its re-solubilization in the intestinal fluid compared to the pure powder and the disaggregated tablet.

3.2.4. *Weak-base drugs (DOM, OLZ & CIN)*

The commercial tablet containing DOM exhibited slower solubilization kinetics in the gastric phase compared to the raw drug (Fig. 3C), as the tablet must disintegrate before the API becomes available. In FaSSIF its behavior is similar to neat DOM and DOM + NaDES with a slight tendency to precipitate.

For OLZ, the test was conducted under sink conditions for the first 60 min, followed by non-sink conditions for the next two hours at intestinal pH. In the gastric phase, the profiles of the raw API and the tablet reached different concentrations in the first 15 min. Specifically, the pure drug solubilized faster than the commercial tablet. On the contrary, the loaded NaDES reached a concentration close to 90 % of the total after 5 min, and it remained constant throughout the gastric phase. In the unfavorable environment, all three profiles maintained a supersaturated state despite a slow recrystallization of OLZ, with a slight reduction of 5–8 % of the total over the next 120 min (Fig. 3D).

For CIN, the profiles of raw CIN and the commercial tablet were substantially overlapping in FaSSGF, showing slow solubilization kinetics during the first 15 min. In contrast, CIN + NaDES achieved

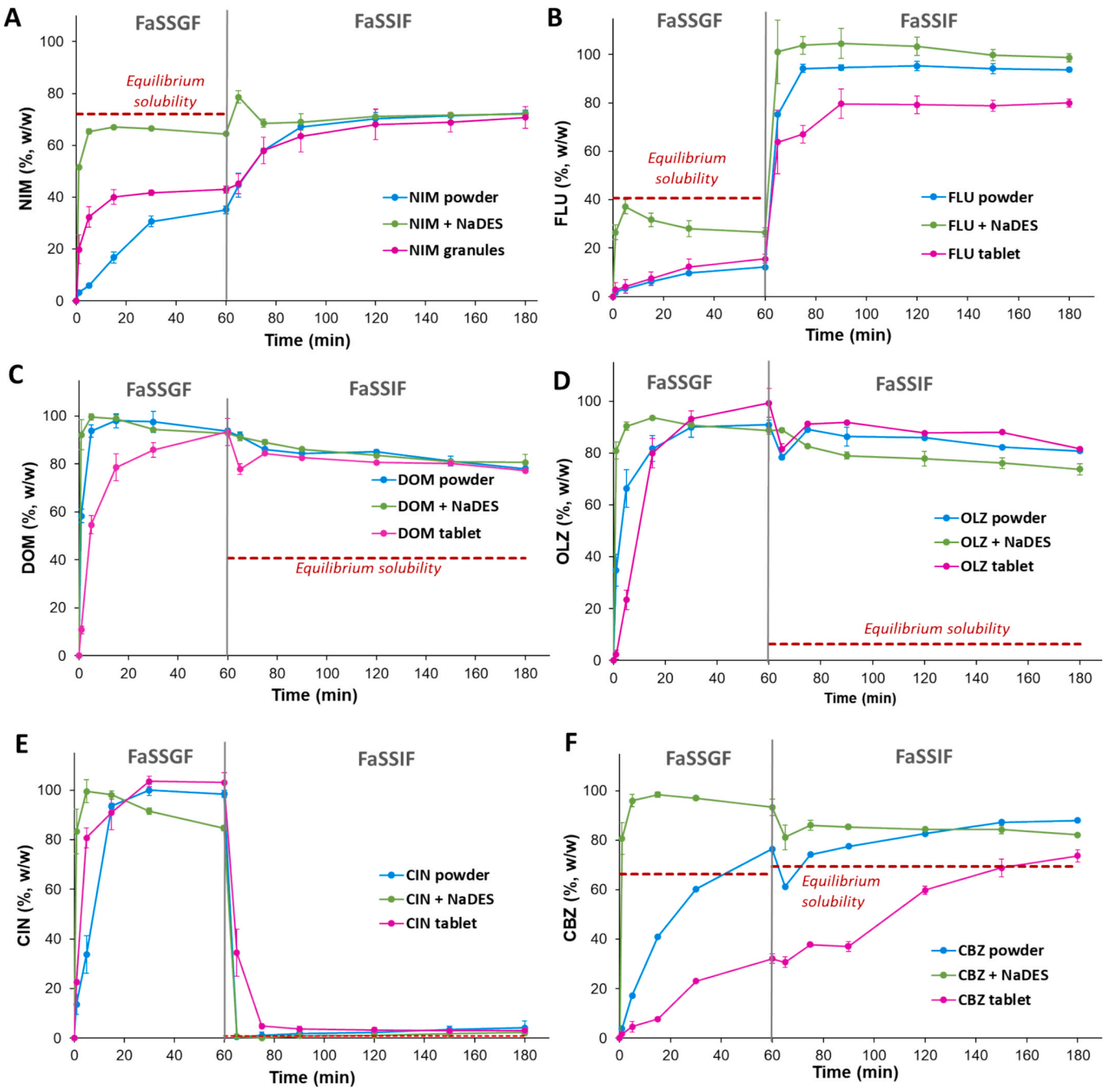

Fig. 3. Dilution profiles of A) NIM, B) FLU, C) DOM, D) OLZ, E) CIN, F) CBZ in NaDES compared to the dissolution profiles of pure drug and of a solid dosage form in biorelevant media. Values are expressed as mean (n = 3) ± SD in % of the total. The vertical green line indicates the time at which the pH change was made. The dotted red line indicates the equilibrium solubility of the neat drug in the considered dissolution medium.

complete solubilization within the first 5 min of the study. After the pH change, the drug immediately precipitated from all samples, reaching a concentration that did not exceed 5 % of the total (Fig. 3E). These results show the close dependence of CIN on pH, making the presence of NaDES and of the FaSSIF surfactants ineffective for maintaining a certain amount of drug in solution in conditions of unfavorable pH. This behavior can likely be explained by its high lipophilicity (log P 5.88) and its structure, which has limited capacity for hydrogen bond formation. Similar findings were reported by Jeliński et al. (2019) who used quantum chemical computations to study interactions between curcumin and a choline chloride–glycerol NaDES. Their study demonstrated that dilution in gastrointestinal fluids led to a marked decrease in curcumin solubility, primarily due to the disruption of stabilizing intermolecular interactions within the eutectic matrix. This occurred despite curcumin's lower lipophilicity (logP ≈ 3.3). A comparable behavior was observed for aprepitant, a weakly basic drug with higher lipophilicity (logP ≈ 5), when solubilized in a NaDES composed of choline chloride and levulinic acid at a 2:1 M ratio (Palmelund et al., 2021). Upon direct addition of aprepitant at doses of 3 mg and 4 mg into 20 mL of FaSSIF, the system maintained an apparent supersaturated state for only 4 and 2 min, respectively, before rapid and extensive precipitation occurred.

3.2.5. *Neutral API (CBZ)*

As shown in Fig. 3F, the raw drug exhibited a faster solubilization kinetics than the tablet, which required disaggregation before

dissolution. This behavior remained consistent throughout the 3-hour testing period. The advantage of the eutectic mixture is extremely evident in this case, as the drug was completely solubilized within the first few minutes and this supersaturated condition was maintained during both the gastric and intestinal phases.

When exposed to water, CBZ is known to undergo phase transformation to the dihydrate, which is less soluble than the stable CBZ form III. Supersaturating drug delivery systems (SDDSs) of CBZ, formulated either as cocrystals or amorphous solid dispersions (ASDs), have been shown to limit this transformation and increased the drug dissolution behavior under non-sink conditions (Thakore et al., 2019). Similarly, the CBZ + NaDES system likely acts as a thermodynamically stable and easily prepared SDDS, offering comparable advantages in maintaining supersaturation and improving solubilization performance.

In summary, these results suggest that performing sequential dilution tests by progressively changing the digestive medium offers a reliable simulation of oral administration, allowing a mechanistic insight into the behavior of DES-based formulations and the fate of drugs with different properties throughout gastrointestinal transit. Specifically, it has been observed that acidic NaDES based on ChCl and MA yield the best outcomes with weak bases having a log P $\leq$ 4 (DOM and OLZ) or pH-independent APIs (CBZ) with a log P $<$ 3. Literature suggests that such compounds, particularly those bearing carboxyl or hydroxyl groups, can engage in hydrogen bonding with the –OH, C═O, and Cl moieties of choline-based NaDES (Mokhtarpour et al., 2020) and even hydrophobic interactions between the methyl groups of the choline cation and the aromatic ring or the aliphatic moiety of the API (Albertini et al., 2023; Karimi et al., 2025; Prabhakar and Ramalingam, 2025; Tussipkan et al., 2025). These interactions likely contribute to the formation of stable supramolecular assemblies, which enhance solubility and may delay precipitation upon dilution, thereby sustaining a supersaturated environment even at critical pH levels. This supersaturation represents the driving force for drug absorption and might offer a significant advantage over solid dosage forms. Conversely, we hypothesize that CIN's high hydrophobicity (log P $>$ 5.5), combined with its limited hydrogen bonding capacity, reduces its ability to remain solubilized in aqueous biorelevant media, especially when the stabilizing NaDES network is disrupted by dilution. These findings support our mechanistic interpretation that the solubility and supersaturation behavior of API + NaDES systems upon dilution are governed by a delicate balance between hydrogen bonding, hydrophobic interactions, and the ability of the drug to remain associated with the NaDES matrix in the presence of competing solubilizing agents (e.g., bile salts, phospholipids) in biorelevant media.

In case of weak acid APIs, the deep eutectic mixture allowed to approach the solubility limit of the API in the digestion model but not to exceed it. Nevertheless, their better solubilization kinetics compared to the pure drug and solid forms (e.g., granules or tablets) may still improve drug in vivo absorption by maintaining a high concentration gradient.

3.3. *In vitro permeability tests*

For each drug, permeability tests of the API + NaDES and the corresponding diluted drug powder were conducted in PBS, FaSSIF, and FeSSIF. The API powder served as a reference to highlight potential advantages related to the presence of NaDES in terms of drug absorption. To calculate the apparent permeability (P_{app}) it is essential to accurately determine the concentration of the free drug fraction (di Cagno and Luppi, 2013; Holzem et al., 2024). However, in our samples, a portion of the drug may remain insolubilized or may be complexed with micelles present in the biorelevant media and/or with NaDES components, making precise quantification of the free drug concentration unfeasible. Therefore, we opted to report the in vitro fraction of dose absorbed (F_abs %), which provides a more practical and representative measure of permeability under these experimental conditions.

3.3.1. *Weak acid drugs*

Permeability studies of weak acid drugs (FLU and NIM) were performed both with NaDES and drug powder in different media (PBS, FaSSIF, FeSSIF). As shown in Fig. 4A, B, the F_{abs} (%) of both samples in the three media exhibited similar trends. In particular, it was demonstrated that the powder suspension of the drug lead to a higher permeation compared to the eutectic mixture.

Nevertheless, FLU and NIM do not exhibit identical behavior. In fact, during FLU tests, a significant difference emerged between the drug absorption in the presence and absence of NaDES. In the former case, Fabs (%) in PBS, FaSSIF, and FeSSIF was almost the same in the three media, suggesting that the pH decrease caused by the presence of NaDES (Table 4) is mainly responsible for the precipitation of the API, limiting its absorption. Concerning raw FLU, Fabs (%) determined in the three media appeared coherent with their pH and composition. In fact, the drug is mostly soluble in FaSSIF rather than PBS and FeSSIF.

For NIM, the differences in the presence and absence of NaDES are less marked but still significant both in PBS ($p < 0.05$) and in FeSSIF ($p < 0.002$). This could be related to the fact that NIM seemed to have a neutral drug-like behavior, as mentioned above.

3.3.2. *Weak base drugs*

Permeability studies of weak base drugs (OLZ, DOM and CIN) show that the F_{abs} (%) of API + NaDES are higher than those of the diluted raw drug across all the media considered. All drugs formulated with NaDES exhibited greater permeability in FaSSIF compared to the other two media. This can be attributed to the presence of solubilizing agents that form micelles, which enhance the absorption of drugs that are molecularly dispersed in the NaDES. This aspect has to be evaluated in relation to the pH decrease caused by the addition of the eutectic mixture (Table 4); in fact, the decrease in pH, which is maximal in FaSSIF, represents the optimal condition for basic drugs.

Regarding raw diluted APIs, drug absorption was lower in both PBS and intestinal media. Based on these findings, it can be confirmed that the NaDES mixture provided a clear advantage for the absorption of weakly basic drugs. This benefit is attributed to the NaDES's ability to form and maintain a supersaturated environment, thereby creating favorable conditions that enhance drug solubility.

3.3.3. *Neutral API*

In vitro permeability studies of CBZ revealed comparable behavior in PBS, both in the presence and absence of NaDES; in fact, the amount of drug permeated from both samples was not significantly different. However, the results for the loaded NaDES in intestinal media showed that the F_{abs} (%) was significantly higher compared to the diluted pure drug in both FaSSIF ($p < 0.0001$) and FeSSIF ($p < 0.05$) (Fig. 4F). This confirms the positive effect of NaDES on the bioavailability of CBZ, as observed in the dilution tests.

To summarize, it appears that NaDES enhanced the permeation of basic and neutral compounds. For basic drugs, this might be linked to the pH which generates a higher concentration gradient and a higher flux through the barrier. The most interesting case is the neutral drug, whose solubility and, by consequence, permeability, are unaffected by pH.

In this scenario, the presence of NaDES provides a clear benefit,

Table 4
Ph values of dissolution media following addition of apis and nades samples.

	PBS (pH 7.4)	FaSSIF (pH 6.5)	FeSSIF (pH 5.00)
NIM + NaDES	4.98	1.64	2.07
FLU + NaDES	5.01	1.60	2.05
DOM + NaDES	5.02	1.67	2.06
CIN + NaDES	5.00	1.63	2.02
OLZ + NaDES	5.04	1.65	2.05
CBZ + NaDES	4.99	1.62	2.00

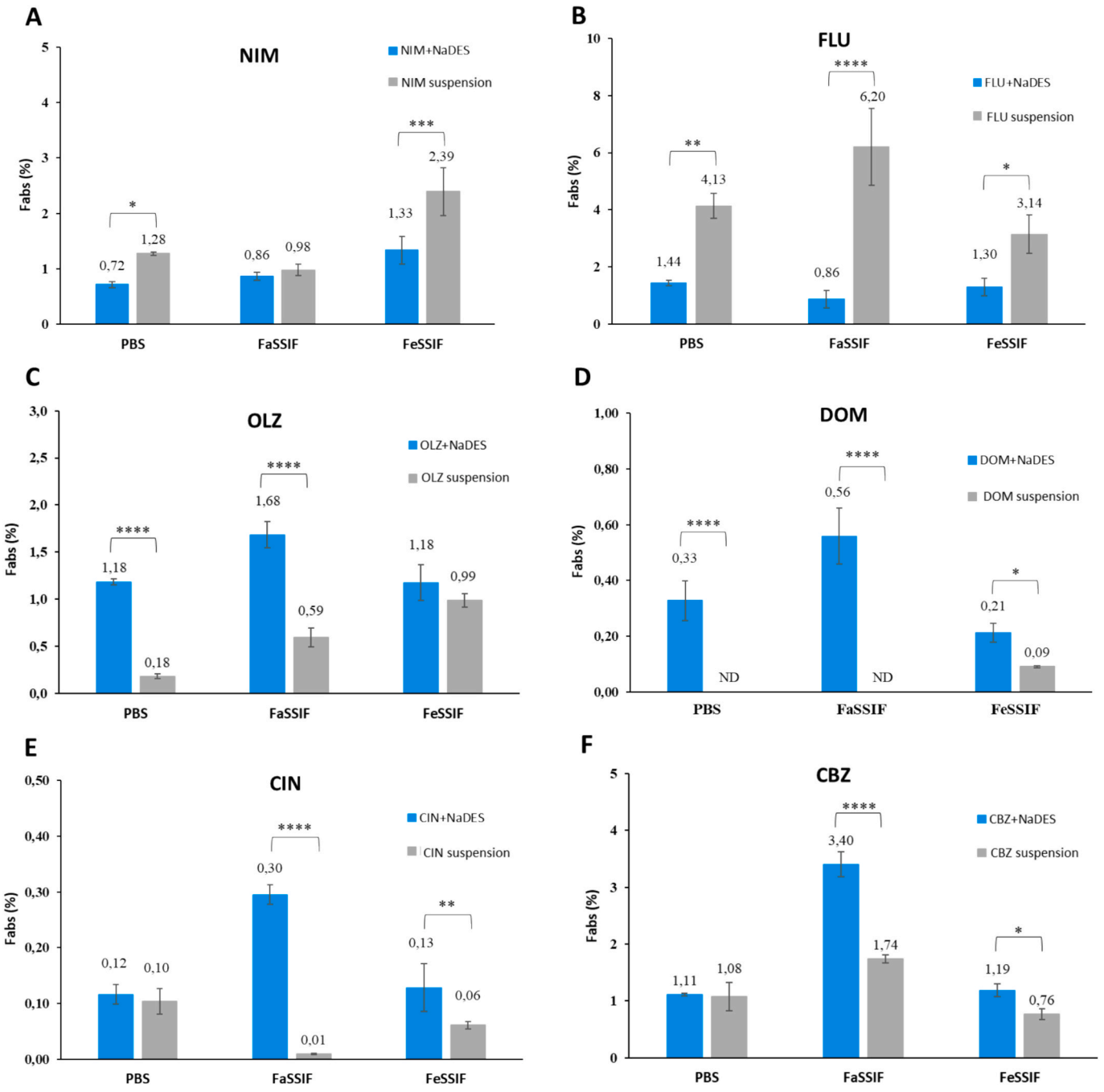

Fig. 4. F_{abs} (%) after 4 h of A) NIM, B) FLU, C) OLZ, D) DOM, E) CIN, F) CBZ in NaDES compared to the diluted raw APIs in PBS, FaSSIF and FeSSIF. Values are expressed as mean (n = 3) ± SD. ****p < 0.0001, ***p < 0.002, **p < 0.01, *p < 0.05 significant difference. ND = not detected.

especially under fasted state conditions and potentially in the fed state as well. This advantage consists in NaDES acting as an effective solubilizing agent, creating a supersaturated solution and thereby generating a high concentration gradient. Such a gradient serves as a driving force that enhances drug permeation across biological membranes.

During these tests, measuring the pH of the drug solutions was important for understanding some of the obtained results. pH affects the ionization state of the API and its solubility in a given environment, both of which may influence drug permeation. Table 4 shows the decrease in pH of the media after the addition of the loaded NaDESs, similarly to what was observed during the dilution tests. This pH change is an important consideration for the development of such formulations, as it might also occur in vivo, at least in the upper intestinal tract following gastric emptying. Importantly, for weakly basic drugs, this transient acidity may help prevent premature precipitation upon entry into the intestinal environment. Conversely, weak acids show reduced performance in NaDES, which may limit the applicability of such formulations for these APIs. Safety considerations are also relevant: while the acidic nature of some NaDES formulations could potentially cause mucosal irritation, oral administration in small volumes (e.g., 2.5–5 mL stick-packs) or via capsules minimizes contact. Once in the GI tract, NaDES are quickly diluted and neutralized by endogenous secretions, minimizing irritation and supporting oral administration feasibility. Although intestinal fluids have limited buffering capacity, especially in the fasted state, several studies have shown that it is sufficient to mitigate extreme acidification under hydrodynamic physiological

conditions (Hens et al., 2017; Litou et al., 2020). In the dilution studies the pH was adjusted to 6.8 (buffer) and 6.5 (biorelevant media) to reflect physiological conditions and the use of large volumes helped attenuate the acidifying effect of NaDES. In contrast, permeation studies with small donor volumes (400 μL) exaggerate pH drops, making pH correction impractical. For this reason, this setup does not replicate the hydrodynamic and buffering conditions of the GI tract and therefore cannot be directly extrapolated to in vivo behavior.

4. Conclusions

In this study, the biopharmaceutical properties of eutectic mixtures based on choline chloride and malic acid containing BCS class II drugs with different physico-chemical properties (i.e. log P and pKa) were evaluated in simulated gastrointestinal fluids. The selected NaDES demonstrated its effectiveness as a solvent for all the tested drugs, enhancing their solubility by 1.5 to 80 times compared to their solubility in buffers. In vitro dilution studies in biorelevant media (FaSSGF and FaSSIF) indicated that NaDES not only improved the solubility of these drugs, but also led to the formation of supersaturated solutions at the respective critical pH, which represent the driving force for drug absorption. In particular, the best results were obtained for weak bases (except for the highest hydrophobic CIN) and pH-independent drugs; while for weak acid APIs, a supersaturated environment did not occur. Permeability results using innovative biomimetic membranes (Permeapad®) in PBS and simulated intestinal fluids (FaSSIF and FeSSIF) supported the in vitro dilution findings, demonstrating that NaDES can increase the absorption of weak base and neutral APIs also in biorelevant media, but not for weak acid drug.

In conclusion, the selected NaDES system demonstrated that the bioavailability-enhancing effect is strongly influenced by the dynamic interplay between the physicochemical properties of NaDES and the molecular characteristics of the drug.

CRediT authorship contribution statement

Stefano Sangiorgi: Writing – original draft, Investigation, Data curation. **Matilde Mancinelli:** Investigation. **Serena Bertoni:** Writing – review & editing, Methodology. **Massimiliano Pio Di Cagno:** Writing – review & editing, Methodology. **Nadia Passerini:** Writing – review & editing, Funding acquisition. **Beatrice Albertini:** Writing – review & editing, Writing – original draft, Supervision, Conceptualization.

Funding

This research did not receive any specific grant from funding agencies in the public, commercial, or not-for-profit sectors.

Declaration of competing interest

The authors declare that they have no known competing financial interests or personal relationships that could have appeared to influence the work reported in this paper.

Appendix A. Supplementary data

Supplementary data to this article can be found online at https://doi.org/10.1016/j.ijpharm.2025.126369.

Data availability

Data will be made available on request.

References

Albertini, B., Bertoni, S., Nucci, G., Botti, G., Abrami, M., Sangiorgi, S., Beggiato, S., Prata, C., Ferraro, L., Grassi, M., Passerini, N., Perissutti, B., Dalpiaz, A., 2024. Supramolecular eutectogel as new oral paediatric delivery system to enhance benznidazole bioavailability. Int. J. Pharm. 661, 124417. https://doi.org/10.1016/j.ijpharm.2024.124417.

Albertini, B., Bertoni, S., Sangiorgi, S., Nucci, G., Passerini, N., Mezzina, E., 2023. NaDES as a green technological approach for the solubility improvement of BCS class II APIs: an insight into the molecular interactions. Int. J. Pharm. 634, 122696. https://doi.org/10.1016/j.ijpharm.2023.122696.

Alqahtani, M.S., Kazi, M., Alsenaidy, M.A., Ahmad, M.Z., 2021. Adv. Oral Drug Delivery. Front. Pharmacol. 12, 618411. https://doi.org/10.3389/fphar.2021.618411.

Amaral Silva, D., Davies, N.M., Bou-Chacra, N., Ferraz, H.G., Löbenberg, R., 2022. Update on gastrointestinal biorelevant media and physiologically relevant dissolution conditions. Dissolution Technol. 29, 62–75. https://doi.org/10.14227/DT290222P62.

Banerjee, A., Ibsen, K., Brown, T., Chen, R., Agatemor, C., Mitragotri, S., 2018. Ionic liquids for oral insulin delivery. Proc. Natl. Acad. Sci. 115, 7296–7301. https://doi.org/10.1073/pnas.1722338115.

Bertoni, S., Albertini, B., Ronowicz-Pilarczyk, J., Passerini, N., 2023. Tailoring the release of drugs having different water solubility by hybrid polymer-lipid microparticles with a biphasic structure. Eur. J. Pharm. Biopharm. 190, 171–183. https://doi.org/10.1016/j.ejpb.2023.07.017.

Chakraborty, S., Sathe, R.Y., Chormale, J.H., Dangi, A., Bharatam, P.V., Bansal, A.K., 2023. Effect of Deep Eutectic System (DES) on Oral Bioavailability of Celecoxib: In Silico, In Vitro, and In Vivo Study. Pharmaceutics 15. Doi: 10.3390/pharmaceutics15092351.

Bhalani, D.V., Nutan, B., Kumar, A., Singh Chandel, A.K., 2022. Bioavailability enhancement techniques for poorly aqueous soluble drugs and therapeutics. Biomedicines 10, 2055. https://doi.org/10.3390/biomedicines10092055.

Culen, M., Rezacova, A., Jampilek, J., Dohnal, J., 2013. Designing a dynamic dissolution method: a review of instrumental options and corresponding physiology of stomach and small intestine. J. Pharm. Sci. 102, 2995–3017. https://doi.org/10.1002/jps.23494.

Cysewski, P., Jeliński, T., 2019. Optimization, thermodynamic characteristics and solubility predictions of natural deep eutectic solvents used for sulfonamide dissolution. Int. J. Pharm. 570, 118682. https://doi.org/10.1016/j.ijpharm.2019.118682.

Dai, Y., Witkamp, G.-J., Verpoorte, R., Choi, Y.H., 2015. Tailoring properties of natural deep eutectic solvents with water to facilitate their applications. Food Chem. 187, 14–19. https://doi.org/10.1016/j.foodchem.2015.03.123.

di Cagno, M., Bibi, H.A., Bauer-Brandl, A., 2015. New biomimetic barrier Permeapad™ for efficient investigation of passive permeability of drugs. Eur. J. Pharm. Sci. 73, 29–34. https://doi.org/10.1016/j.ejps.2015.03.019.

di Cagno, M., Luppi, B., 2013. Drug "supersaturation" states induced by polymeric micelles and liposomes: a mechanistic investigation into permeability enhancements. Eur. J. Pharm. Sci. 48, 775–780. https://doi.org/10.1016/j.ejps.2013.01.006.

Faggian, M., Sut, S., Perissutti, B., Baldan, V., Grabnar, I., Dall'Acqua, S., 2016. Natural Deep Eutectic Solvents (NADES) as a tool for bioavailability improvement: pharmacokinetics of rutin dissolved in proline/glycine after oral administration in rats: possible application in nutraceuticals. Molecules 21. https://doi.org/10.3390/molecules21111531.

Hammond, O.S., Bowron, D.T., Edler, K.J., 2017. The effect of water upon deep eutectic solvent nanostructure: an unusual transition from ionic mixture to aqueous solution. Angew. Chem. Int. Ed. 56, 9782–9785. https://doi.org/10.1002/anie.201702486.

Hens, B., Tsume, Y., Bermejo, M., Paixao, P., Koenigsknecht, M.J., Baker, J.R., Hasler, W. L., Lionberger, R., Fan, J., Dickens, J., Shedden, K., Wen, B., Wysocki, J., Loebenberg, R., Lee, A., Frances, A., Amidon, G., Yu, A., Benninghoff, G., Salehi, N., Talattof, A., Sun, D., Amidon, G.L., 2017. Low buffer capacity and alternating motility along the human gastrointestinal tract: implications for in vivo dissolution and absorption of ionizable drugs. Mol. Pharm. 14, 4281–4294. https://doi.org/10.1021/acs.molpharmaceut.7b00426.

Holzem, F.L., Parrott, N., Petrig Schaffland, J., Brandl, M., Bauer-Brandl, A., Stillhart, C., 2024. Oral absorption from surfactant-based drug formulations: the impact of molecularly dissolved drug on bioavailability. J. Pharm. Sci. 113, 3054–3064. https://doi.org/10.1016/j.xphs.2024.07.017.

Jantratid, E., Janssen, N., Reppas, C., Dressman, J.B., 2008. Dissolution media simulating conditions in the proximal human gastrointestinal tract: an update. Pharm. Res. 25, 1663–1676. https://doi.org/10.1007/s11095-008-9569-4.

Jeliński, T., Przybyłek, M., Cysewski, P., 2019. Natural deep eutectic solvents as agents for improving solubility, stability and delivery of curcumin. Pharm. Res. 36, 116. https://doi.org/10.1007/s11095-019-2643-2.

Karimi, N., Heydari Dokoohaki, M., Zolghadr, A.R., Klein, A., 2025. Solvation and aggregation of heteroaromatic drugs in the Reline deep eutectic solvent – a combined molecular dynamics simulation and DFT study. PCCP 27, 15527–15543. https://doi.org/10.1039/D5CP01312G.

Li, Z., Lee, P.I., 2016. Investigation on drug solubility enhancement using deep eutectic solvents and their derivatives. Int. J. Pharm. 505, 283–288. https://doi.org/10.1016/j.ijpharm.2016.04.018.

Litou, C., Psachoulias, D., Vertzoni, M., Dressman, J., Reppas, C., 2020. Measuring pH and buffer capacity in fluids aspirated from the fasted upper gastrointestinal tract of healthy adults. Pharm. Res. 37, 42. https://doi.org/10.1007/s11095-019-2731-3.

Liu, Y., Wu, Y., Liu, J., Wang, W., Yang, Q., Yang, G., 2022. Deep eutectic solvents: recent advances in fabrication approaches and pharmaceutical applications. Int. J. Pharm. 622, 121811. https://doi.org/10.1016/j.ijpharm.2022.121811.

Loisios-Konstantinidis, I., Cristofoletti, R., Jamei, M., Turner, D., Dressman, J., 2020. Physiologically based pharmacokinetic/pharmacodynamic modeling to predict the impact of CYP2C9 genetic polymorphisms, co-medication and formulation on the pharmacokinetics and pharmacodynamics of flurbiprofen. Pharmaceutics 12. https://doi.org/10.3390/pharmaceutics12111049.

Martins, M., Pinho, S., Coutinho, J., 2019. Insights into the nature of eutectic and deep eutectic mixtures. J. Solution Chem. 48. https://doi.org/10.1007/s10953-018-0793-1.

Milián-Guimerá, C., McCabe, R., Thamdrup, L.H.E., Ghavami, M., Boisen, A., 2023. Smart pills and drug delivery devices enabling next generation oral dosage forms. J. Controlled Release 364, 227–245. https://doi.org/10.1016/j.jconrel.2023.10.041.

Mokhtarpour, M., Shekaari, H., Shayanfar, A., 2020. Design and characterization of ascorbic acid based therapeutic deep eutectic solvent as a new ion-gel for delivery of sunitinib malate. J. Drug Delivery Sci. Technol. 56, 101512. https://doi.org/10.1016/j.jddst.2020.101512.

Morrison, H.G., Sun, C.C., Neervannan, S., 2009. Characterization of thermal behavior of deep eutectic solvents and their potential as drug solubilization vehicles. Int. J. Pharm. 378, 136–139. https://doi.org/10.1016/j.ijpharm.2009.05.039.

Moshikur, R.M., Carrier, R.L., Moniruzzaman, M., Goto, M., 2023. Recent advances in biocompatible ionic liquids in drug formulation and delivery. Pharmaceutics 15. https://doi.org/10.3390/pharmaceutics15041179.

Mustafa, N.R., Spelbos, V.S., Witkamp, G.-J., Verpoorte, R., Choi, Y.H., 2021. Solubility and stability of some pharmaceuticals in natural deep eutectic solvents-based formulations. Molecules 26. https://doi.org/10.3390/molecules26092645.

Omar, K.A., Sadeghi, R., 2022. Physicochemical properties of deep eutectic solvents: a review. J. Mol. Liq. 360, 119524. https://doi.org/10.1016/j.molliq.2022.119524.

Palmelund, H., Eriksen, J.B., Bauer-Brandl, A., Rantanen, J., Löbmann, K., 2021. Enabling formulations of aprepitant: in vitro and in vivo comparison of nanocrystalline, amorphous and deep eutectic solvent based formulations. Int. J. Pharm.: X 3, 100083. https://doi.org/10.1016/j.ijpx.2021.100083.

Peng, K., Gao, Y., Angsantikul, P., LaBarbiera, A., Goetz, M., Curreri, A.M., Rodrigues, D., Tanner, E.E.L., Mitragotri, S., 2021. Modulation of gastrointestinal mucus properties with ionic liquids for drug delivery. Adv. Healthc. Mater. 10, 2002192. https://doi.org/10.1002/adhm.202002192.

Prabhakar, P., Ramalingam, A., 2025. Influence of functional groups on drug solubility using choline chloride-based deep eutectic solvents. J. Mol. Model. 31, 263. https://doi.org/10.1007/s00894-025-06474-w.

Rozas, S., Benito, C., Alcalde, R., Atilhan, M., Aparicio, S., 2021. Insights on the water effect on deep eutectic solvents properties and structuring: The archetypical case of choline chloride + ethylene glycol. J. Mol. Liq. 344, 117717. https://doi.org/10.1016/j.molliq.2021.117717.

Saiswani, K., Narvekar, A., Jahagirdar, D., Jain, R., Dandekar, P., 2023. Choline chloride: glycerol deep eutectic solvents assist in the permeation of daptomycin across Caco-2 cells mimicking intestinal bilayer. J. Mol. Liq. 383, 122051. https://doi.org/10.1016/j.molliq.2023.122051.

Sangiorgi, S., Albertini, B., Bertoni, S., Passerini, N., 2025. An overview on the role of ionic liquids and deep eutectic solvents in oral pharmaceuticals. Pharmaceutics 17. https://doi.org/10.3390/pharmaceutics17030300.

Schver, G.C.R.M., Lee, P.I., 2021. On the usefulness of sink index in characterizing the degree of nonsinkness in dissolution studies. Int. J. Pharm. 605, 120845. https://doi.org/10.1016/j.ijpharm.2021.120845.

Smith, E.L., Abbott, A.P., Ryder, K.S., 2014. Deep Eutectic Solvents (DESs) and their applications. Chem. Rev. 114, 11060–11082. https://doi.org/10.1021/cr300162p.

Sut, S., Faggian, M., Baldan, V., Poloniato, G., Castagliuolo, I., Grabnar, I., Perissutti, B., Brun, P., Maggi, F., Voinovich, D., Peron, G., Dall'Acqua, S., 2017. Natural Deep Eutectic Solvents (NADES) to enhance berberine absorption: an in vivo pharmacokinetic study. Molecules 22. https://doi.org/10.3390/molecules22111921.

Thakore, S.D., Thakur, P.S., Shete, G., Gangwal, R., Narang, A.S., Sangamwar, A.T., Bansal, A.K., 2019. Assessment of biopharmaceutical performance of supersaturating formulations of carbamazepine in rats using physiologically based pharmacokinetic modeling. AAPS PharmSciTech 20, 179. https://doi.org/10.1208/s12249-019-1386-z.

Tussipkan, D., Chaohua, C., Aidarkhan, K., Caisheng, Q., Xixia, S., Lili, T., Dandan, L., Toktarbay, Z., Zhalel, A., Manabayeva, S., 2025. Atomistic insights into the intermolecular interactions of Cistanoside a from Cistanche deserticola with natural deep eutectic solvents. Discover Appl. Sci. 7, 956. https://doi.org/10.1007/s42452-025-07553-6.

Vertzoni, M., Fotaki, N., Nicolaides, E., Reppas, C., Kostewicz, E., Stippler, E., Leuner, C., Dressman, J., 2010. Dissolution media simulating the intralumenal composition of the small intestine: physiological issues and practical aspects. J. Pharm. Pharmacol. 56, 453–462. https://doi.org/10.1211/0022357022935.

Zainal-Abidin, M.H., Hayyan, M., Ngoh, G.C., Wong, W.F., Looi, C.Y., 2019. Emerging frontiers of deep eutectic solvents in drug discovery and drug delivery systems. J. Control. Release 316, 168–195. https://doi.org/10.1016/j.jconrel.2019.09.019.

Zhuo, Y., Cheng, H.-L., Zhao, Y.-G., Cui, H.-R., 2024. Ionic liquids in pharmaceutical and biomedical applications: a review. Pharmaceutics 16. https://doi.org/10.3390/pharmaceutics16010151.